Journal of the Korean Institute of Illuminating and Electrical Installation Engineers Vol. 23, No.7, pp. 29~40 July 2009 (23-7-5)

Control and Operation of Hybrid Microsource System Using Advanced Fuzzy-Robust Controller

Won-Pyo Hong* · Hee-Sang Ko

Abstract

This paper proposes a modeling and controller design approach for a hybrid wind power generation system that considers a fixed wind-turbine and a dump load. Since operating conditions are kept changing, it is challenge to design a control for reliable operation of the overall system. To consider variable operating conditions, Takagi-Sugeno (TS) fuzzy model is taken into account to represent time-varying system by expressing the local dynamics of a nonlinear system through sub-systems, partitioned by linguistic rules. Also, each fuzzy model has uncertainty. Thus, in this paper, a modern nonlinear control design technique, the sliding mode nonlinear control design, is utilized for robust control mechanism. In the simulation study, the proposed controller is compared with a proportional-integral (PI) controller. Simulation results show that the proposed controller is more effective against disturbances caused by wind speed and load variation than the PI controller, and thus it contributes to a better quality wind-hybrid power generation system.

Key Words : Wind Power Generation, Dump Load, Takagi-Sugeno Fuzzy Model, Sliding Mode Control

1. Introduction

To supply electricity to islands or isolated communities, combining wind power with diesel generator sets seems to be an attractive solution economically. Considerable fuel savings can be achieved by utilizing wind power, but due to the fluctuating nature of the wind, there arise several technical problems concerning power quality. The drawback of wind power generation is its dependence on nature-power output varies widely due to changes in wind speed, which are difficult to model and predict. Excessive fluctuation of power output negatively influences the quality of electricity, particularly frequency and voltage, in small-scale system such as in islands and in remote areas[1-2].

A hybrid system is generally composed of a wind-turbine coupled with an induction generator, an energy storage system, a dump load, and a backup diesel engine-driven synchronous generator for operation when wind power is insufficient. There can be several possible modes of operation in this hybrid system [3-13]. Most published works [3-9] relate to situations wherein wind-generated power is not sufficient to meet the

* Main author : professor of the Department of Building Services Engineering at the Hanbat National University
Tel : +82-42-821-1179, Fax : +82-42-821-1175
E-mail : wphong@hanbat.ac.kr
Date of submit : 2009. 4. 24
First assessment : 2009. 4. 30
Completion of assessment : 2009. 6. 1

load. Therefore, a diesel engine is employed as a backup, resulting in a so-called wind-diesel hybrid system. Other works [10-13] utilize an energy storage system before adding a diesel engine to the system.

This paper considers a mode where both the wind turbine-induction generator unit and the dump load operate in parallel. In this mode, wind-generated power is sufficient to supply loads and the diesel engine is disconnected from the synchronous generator.

The synchronous generator acts as a synchronous condenser, to generate or absorb the reactive power that contributes to its terminal voltage in stabilizing the system. The dump load is applied to the frequency control by absorbing the excess active power in the network. Since no dynamic model of a wind-dump load system has been reported, this paper develops a novel nonlinear dynamic model of a wind-dump load system. In power systems, the voltage and frequency are mainly dependent on reactive power and active power, respectively. When the frequency is very stable [14], it does not affect voltage. However, there are two main problems with remote wind hybrid system installations. One is that overall system inertia is relatively small; consequently, the system is sensitive to disturbances such as wind speed and load variations. The other is that wind turbines drive induction generators. Wind power changes reactive power consumption as well as active power generation from the induction generator; therefore, variations occur in voltage as well as in frequency. These variations interact with the system and degrade power quality. These systems are coupled, in that every input controls more than one output, and every output is controlled by more than one input. Thus, a special control strategy has to be considered for this multi-input-multi-output system. To do that, the sliding mode control is applied because it is a multivariable controller and provides robustness against uncertainties and disturbances [15]. The nonlinear model is reduced for the purpose of designing the controller. With a reduced-order model, the proposed controller is designed based on the sliding mode control and the TS fuzzy model [16]. The TS fuzzy model provides a simple and straightforward way to decompose the task of modeling and controller design into a group of local tasks, which tend to be easier to handle and, in the end, the TS fuzzy model also provides the mechanism to blend these local tasks together to deliver the overall model and control design. Therefore, by employing the TS fuzzy model, we devise a control methodology to take advantage of the advances of modern control. In the simulation study, the proposed controller is compared with the proportional-integral (PI) controller [17].

This paper is divided into 5 sections, beginning with the introduction, in Section I. In Section II, the wind-dump load mode is modeled. Based on the reduced-order model, the proposed controller is developed in Section III. In Section IV, the controller is evaluated in various simulation studies, and conclusions are drawn in Section V.

2. System Model

A wind-dump load hybrid system consists of a wind turbine, an induction generator (IG), a diesel engine (DE), a synchronous generator (SG), a dump load, and a load. The DE is disconnected from the SG by an electromagnetic clutch. A three-phase dump load is used with each phase consisting of seven transistor-controlled resistor banks [2]. The mathematical models of the system components are derived and given in Appendix A. Fig. 1 shows the structure of a wind-dump load

system: e_{fd} is the excitation field voltage, f is the frequency, V_b is the bus voltage, C_a is the capacitor bank, P_{dump} is the required dump load power, and r_{dump} is the dump load resistance.

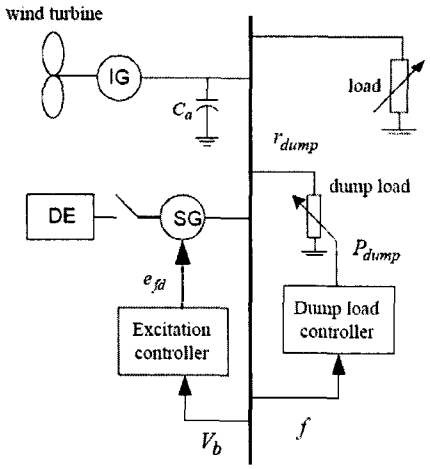

Fig. 1. The overall control structure of a wind-dump load system.

3. Fuzzy-robust Controller Design

The proposed controller is design based on the state feedback approach. In practical systems, it is difficult or impossible to measure all states as required. Therefore, special considerations are needed when a controller is designed, based on state feedback.

In this paper, two considerations are made for a controller design: first, a reduced-order nonlinear model is derived to describe the nonlinear system with only target states, which are easily measurable. Second, an extended state-space model is presented to overcome a non-zero final state problem because the state feedback approach is usually based on the zero final states. For a non-zero final state, an output feedback and a state observer approach are normally used [17-20]. The design procedure presented in this paper, however, is simpler than the output feedback and state observer approaches. Fig. 2 depicts the input and output relationship of the wind-dump load system from the control point of view.

The control inputs are the excitation field voltage (u1) of the SG and the dump load resistance (u2). The measurements are the voltage amplitude (y1) and the frequency (y2) of the AC bus. The wind speed (v1) and load (v2) are considered to be disturbances. The wind turbine generator and the dump load run in parallel, serving the load. From the control point of view, this is a coupled 2×2 multi-input-multi-output nonlinear system, since every input controls more than one output and every output is controlled by more than one input.

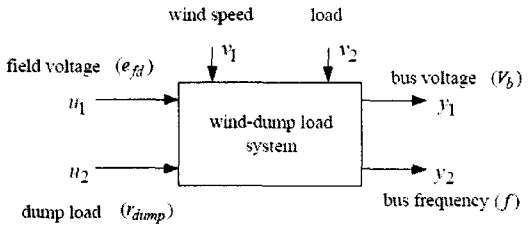

Fig. 2. The wind-dump load control system.

3.1 Model Evaluation

The models of the generators are based on the standard Park's transformation [21] that transforms all stator variables to a rotor reference frame described by a direct and quadratic (d-q) axis. The set of SG equations are based on the d-q axis in accordance with [22]. The nonlinear mathematical model of the wind-dump load system is described in detail in Appendix A. The following considerations are taken into account to identify component models: the electrical system is assumed as a perfectly balanced three-phase system with pure sinusoidal voltage and frequency. High frequency transients in stator

variables are neglected, which indicates that the stator voltage and currents are allowed to change instantly, because this paper is focused on the transient period instead of sub-transient period. Damper-winding models are ignored because their effect appears mainly in a grid-connected system or a system with several synchronous generators running in parallel. The different component models are of equal level of complexity. Finally, the models reflect the main dynamic characteristics that are important from control point of view. Thus, the models selected are suitable for analysis of relatively small-scale power systems in contrast to large grid-connected systems.

3.2 Dump Load Model

Fig. 3 is the three-phase dump load, where each phase consists of 7 transistor-controlled resistor banks with binary resistor sizing in order to minimize quantum effects and provide more-or-less linear resolution. Fig. 4 shows how the transistors are switched to meet the required power. For example, based on the rated AC line voltage of 230[V] and per-phase resistance of R (=120[Ω]), if the required dump load power from the dump load controller is 880[W], Step-2 is identified, and only switch S2 is turned ON.

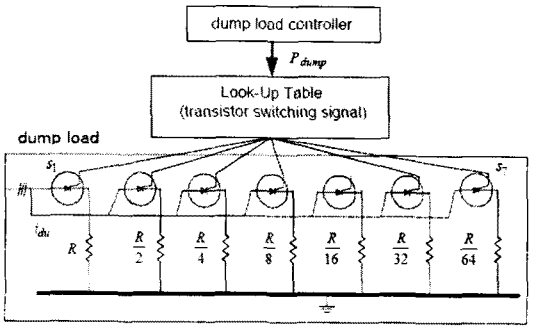

Fig. 3. The structure of the dump load with

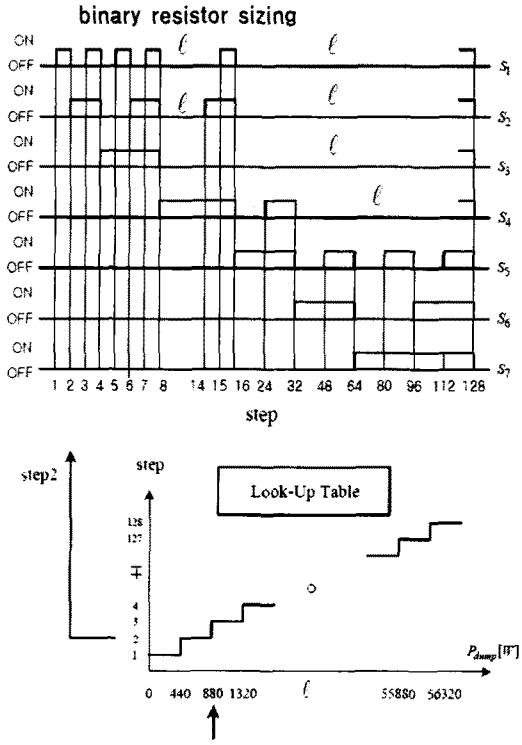

Fig. 4. Transistor switching signal

3.3 Reduced-order Model

The nonlinear mathematical model of the wind-dump load system described in Appendix A is reduced to the following second-order model, to be used for a controller design:

$$\tilde{\omega}_s = \frac{1}{J_s}(-D_s\omega_s - T_s)$$
$$\tilde{\psi}_f = \frac{1}{\tau'_{do}}(-\psi_f + L_{md}i_{sd}) + e_{fd} \quad (1)$$

A reduced-order model is based on the following assumptions: the tortional modes of the mechanical drive trains are assumed to be outside of the desired bandwidth of the controlled system, there is no elasticity in the drive train, and electrical dynamics of the induction generator are not explicitly modeled.

A complete list of symbols is given in Appendix A.

The reduced-order model (1) can be slightly modified to present dump load effect in the system by noting that the air gap torque of the synchronous generator Ts can be represented as

$$T_s = \frac{P_s}{\omega_s} = \frac{P_{dump} + P_{load} - P_{ind}}{\omega_s} \tag{2}$$

where P_{dump}, P_s, and P_{ind} are the power of dump load, the synchronous generator, and the induction generator, respectively, and ωs is the angular speed, which is proportional to frequency f.

Applying (2) into (1), the reduced-order model becomes

$$\begin{aligned} \tilde{\omega}_s &= \frac{1}{J_s}\left(-D_s\omega_s + \frac{P_{ind} - P_{load}}{\omega_s} - \frac{1}{\omega_s}P_{dump}\right) \\ \tilde{\psi}_f &= \frac{1}{\tau'_{do}}(-\psi_f + L_{md}i_{sd}) + e_{fd} \end{aligned} \tag{3}$$

In (3), flux linkage ψf can be modified in terms of the bus voltage and the frequency. This is because, in local operating point, the following assumption can be made such that the rate of change of voltage is a linear combination of the rate of change of rotor flux and angular speed of the SG:

$$\tilde{V}_b = \eta_1\tilde{\psi}_f + \eta_2\tilde{\omega}_s \tag{4}$$

where $\eta_1 = \frac{\partial V_b}{\partial \psi_f}$ and $\eta_2 = \frac{\partial V_b}{\partial \omega_s}$. Here, η1 and η2 are approximated as 1 [p.u.]. Therefore, from (3) and (4) the final reduced-order model is derived as

$$\begin{aligned} \tilde{x}(t) &= Ax(t) + Bu(t) \\ y(t) &= Cx(t) \end{aligned} \tag{5}$$

where $x(t) = [V_b\ \omega_s]^T$, $u(t) = [e_{fd}\ P_{dump}]^T$,

$$A = \begin{bmatrix} 1 & 1 \\ 0 & 1 \end{bmatrix}\begin{bmatrix} -\frac{L_f}{T'_{do}L_{md}\omega_s} & \frac{L_f}{T'_{do}\omega_s L_{md}}\left(L_d i_{sd} - \frac{r_a i_{sq}}{\omega_s}\right) \\ \frac{P_{ind} - P_{load}}{J_s V_b \omega_s} & -\frac{D_s}{J_s} \end{bmatrix}$$

$$B = \begin{bmatrix} 1 & -\frac{1}{J_s\omega_s} \\ 0 & -\frac{1}{J_s\omega_s} \end{bmatrix}, C = \begin{bmatrix} 1 & 0 \\ 0 & 1 \end{bmatrix}$$

Note that the model (5) is in the linear form for fixed system matrices A, B and C. However, matrices A and B are not fixed, but changes as functions of state variables, thus making the model nonlinear. Therefore, even though the reduced-order model is used to design a controller, the TS fuzzy-model based controller can be designed taking into account model imperfections and uncertainties. The proposed controller is designed in the following sub-sections.

3.4 Fuzzy-robust Controller

The main feature of the Takagi-Sugeno fuzzy model expresses the local dynamics of a nonlinear system through linear sub-systems partitioned by linguistic rules. Therefore, by employing the TS fuzzy model, modern linear control theory can be utilized in devising a control methodology for the nonlinear system. In this paper, three linear sub-systems are considered as the state-space model:

$$\begin{aligned} \tilde{x}(t) &= A_i x(t) + B_i u(t) \\ y(t) &= C_i x(t) \quad , i = 1,2,3 \end{aligned} \tag{6}$$

where $A_i \in \Re^{n\times n}$, $B_i \in \Re^{n\times m}$, and $C_i \in \Re^{p\times n}$ Here, n, m, and p are the number of states, inputs, and outputs, respectively. It can be seen from the

reduced model (5) that n=m=p=2. The sub-systems are obtained by partitioning the state-space into overlapping ranges of low, medium, and high states. For each sub-space, different model (i=1, 2, 3) is applied. The degree of membership function for each state-space is depicted in Fig. 5. Here, LP(i=1), BP(i=2), and HP(i=3) stand for possible low, most possible, and possible high membership functions, respectively. Each membership function also represents model uncertainty for each sub-system. The implicit rule is to apply corresponding sub-systems according to the degree of belongings to each sub-space measured by the membership functions. Therefore, even if the sub-systems are linear model, the composite system represents the nonlinear system.

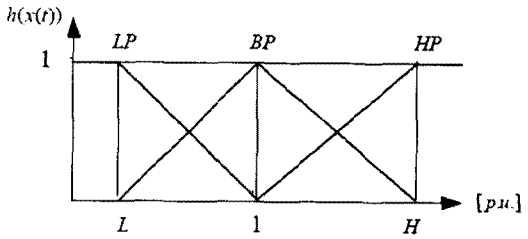

Fig. 5. The membership function for states

Three controllers are designed for three linear sub-systems, after which the final controller output is obtained by defuzzification. When the three controllers are obtained for each sub-system, each control input is weighted by its own membership function shown in Fig. 5. The fuzzy-robust controller output is then obtained by defuzzification as

$$u_{FR}(t)=\frac{\sum_{i=1}^{3} h_i(x(t))u_i(t)}{\sum_{i=1}^{3} h_i(x(t))} \quad (7)$$

where $u_{FR}(t)$ is the fuzzy-robust controller output, $u_i(t)$ is the controller output for each linear sub-system, and $h_i(x(t))$ is the membership value of each linear sub-system.

3.5 Non-zero Final States

Omitting the subscripts in (6) for convenience, the state-space model for each sub-system is given as:

$$\dot{x}(t)=Ax(t)+Bu(t),\quad y(t)=Cx(t) \quad (8)$$

The conventional linear control law based on the state feedback applies to zero final states. However, the final states may not be zero but constants, such as in the system under study. Therefore, it is necessary to consider the tracking problem.

Here, to address the tracking problem an additional state

$x(t)\in\Re^{p}$ is introduced as

$$\dot{x}_r(t)=r(t)-y(t), \quad (9)$$

Where, the signal r(t) satisfies

$$\dot{r}(t)=\gamma(r(t)-r_{ref}) \quad (10)$$

with a positive definite design matrix $\gamma\in\Re^{P\times P}$, and a constant reference vector $r_{ref(=1)}$.

Equation (9) utilizes the integral action in (10) that makes the steady-state error become zero. Therefore, when the initial state x(0) is non-zero, the signal r(t) makes the state $x_r(t)$ zero. Hence, the non-zero final state problem can be solved.

Augmenting with the additional state, the states are now defined as

$$\tilde{x}(t) = [x_r(t) \quad x(t)]^T \tag{11}$$

Where, $\hat{x}(t) \in \Re^{p+n}$ is the augmented state, and the associated augmented system is represented as

$$\dot{\tilde{x}}(t) = \hat{A}\hat{x}(t) + \hat{B}u(t) \tag{12}$$

where $\hat{A} \in \Re^{(p+n)\times(p+n)}, \hat{B} \in \Re^{(p+n)\times m}$ and

$$\hat{A} = \begin{bmatrix} 0 & -c \\ 0 & A \end{bmatrix}, \quad \hat{B} = \begin{bmatrix} 0 \\ B \end{bmatrix}$$

The proposed controller is derived based on the augmented matrices in (12). The signal r(t) will be added in the final control structure.

3.6 Sliding Mode Controller

To design a controller for each sub-system, the sliding mode control is applied that provides robustness against disturbances and uncertainties [15].

The sliding mode controller is a multivariable controller designed by minimizing the following quadratic performance index [17] with the state-space model of (12):

$$J = \frac{1}{2}\int_0^\infty \hat{x}(t)^T Q\hat{x}(t)dt \tag{13}$$

Where, Q is a symmetric-positive definite matrix.

The linear controller for each linear sub-system (7) can be designed as

$$u(t) = -(S\tilde{B})^{-1}(S\tilde{A} - \xi S)\hat{x}(t) \tag{14}$$

where, S is the hyperplane system matrix and where $\xi \in \Re^{m\times m}$ is a stable design matrix. The detailed design procedure is given in Appendix B.

The overall proposed control scheme is given in Fig. 6. Here, $u_F(t)$ is the final control input in the form

$$u_F(t) = r(t) + u_{FR}(t) \tag{15}$$

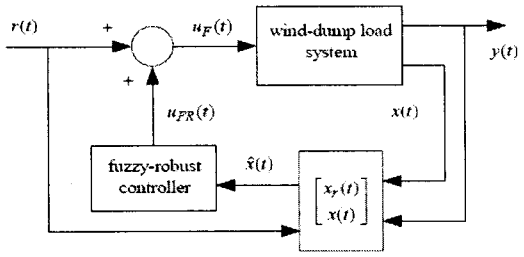

Fig. 6. The overall wind-dump load control scheme

4. Evaluation by Simulation

4.1 System Parameters

The system under study consists of a horizontal axis, 3-bladed, stall regulated wind turbine with a rotor of 16.6[m] diameter that drives an induction generator (IG) rated at 55[kW]. The IG is connected to an AC bus in parallel with a diesel-synchronous generator unit. This unit consists of a 50[kW] turbocharged diesel engine (DE) driving a 55[kVA] brushless synchronous generator (SG). Nominal system frequency is 50[Hz], and the rated line AC voltage is 230[V] [4]. However, in this study the DE is disconnected and the SG is used as a synchronous condenser. The dump load consists of seven transistor-controlled resistor banks, rated at 55[kW]. Load is rated at 40[kW]. The rated wind speed is 7.25[m/s]. The inertia of the induction generator is 1.40[kgm^2] and the inertia of the synchronous generator is 1.11[kgm^2].

This section describes a simulation performance that tests the proposed controller. The augmented system state $\hat{x}(t)$ is defined as

$$\hat{x}(t) = [x_{r,1}(t) \;\; x_{r,2}(t) \;\; x_1(t) \;\; x_2(t)]^T \qquad (16)$$

where x_1 and x_2 stand for voltage and frequency, respectively.

Three linear models are obtained from (6) applying L=0.5 and H=1.5 for both V_b and f. For controller design parameters, the diagonal matrix Q is with $Q_b V_{11}=Q_{33}=1000$ and $Q_{22}=Q_{44}=2000$, and the diagonal matrix ξ is with $\xi_{11}=50$ and $\xi_{22}=80$. The rest of the terms equal zero. The tuned PI controller gains for the governor and excitation system are $P_{gov}=20$, $I_{gov}=60$, and $P_{efd}=30$, $I_{efd}=90$.

4.2 Wind-dump Load Control

Wind speed is shown in Fig. 7. For the simulation task, a step load change is applied at 5 seconds from the initial loading of 35[kW] to 27[kW]. In the following figures, the proposed fuzzy-robust controller is referred to as SMLQR for comparison with the PI controller. Fig. 8 shows the power in the IG, the load, and the dump load. In this case, when the load decreases, the dump load dissipates the excess power in the network.

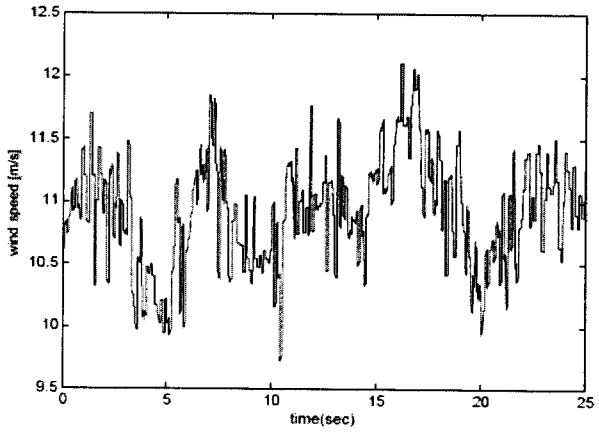

Fig. 7. Wind speed variations

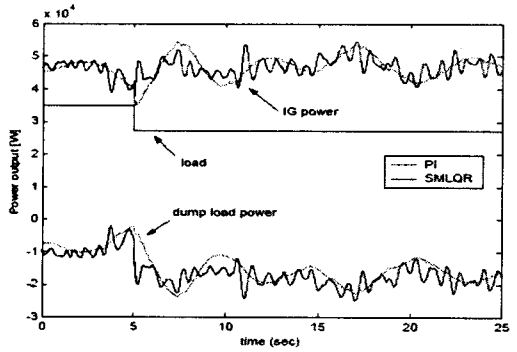

Fig. 8. Power outputs of IG, load and dump load

The proposed control scheme improves the bus frequency performance compared to the PI controller as shown in Fig. 9.

In this system, the SG is used as a synchronous condenser. By controlling the field excitation, the SG can be made to either generate or absorb reactive power to maintain its terminal voltage.

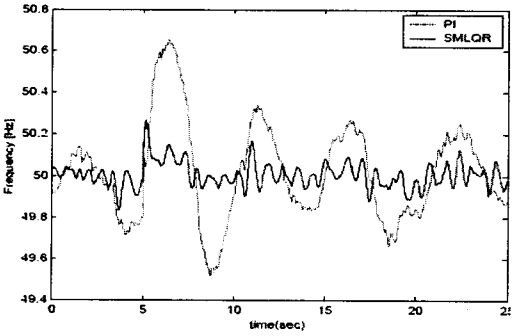

Fig. 9. Frequency performance

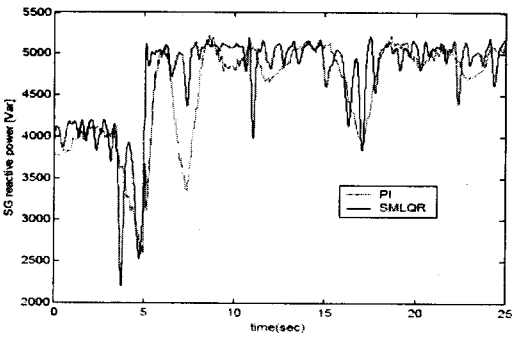

Fig.10. Reactive power output from the SG

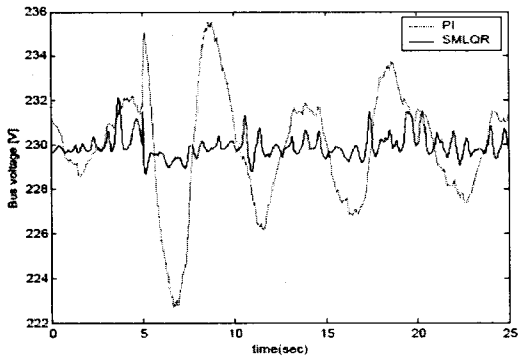

Fig. 11. Bus voltage performance

In SMLQR, the improvement of frequency and voltage with respected to the PI controller is 51.922[%] and 52.511[%] in per unit, respectively. The fuzzy-robust controller achieves better performance compared to the PI controller. The maximum voltage and frequency deviations are less than 1[%]. However, the voltage performance of the PI controller shows slow damping. Such poor performance is caused by the neglect of the interaction of variables between the PI controller loops [23]. Clearly, a control method is required that handles a multi-input-multi-output system. In the proposed controller, all performances are smooth and damped. Therefore, the fuzzy-robust controller provides more effective mechanism for multi-input-multi-output nonlinear system.

5. Conclusions

In this paper, the modeling of a wind-dump load system has been presented for power quality analysis, and the proposed control scheme is derived based on the Takagi-Sugeno (TS) fuzzy model and the sliding mode control. The proposed state-space model provides a new means for a controller design, especially when system states are not fully measurable or a non-zero final state. By employing the TS fuzzy model that represents a nonlinear system with several linear sub-systems, combined by linguistic rules, and by using the sliding mode control for each sub-system, the TS fuzzy model based controller can be designed taking into account model imperfections and uncertainties even though the reduced-order model is used to design a controller. The proposed controller provides more effective control for the system to achieve good power quality, which is demonstrated by smooth transition of bus voltage and frequency.

6. Appendix

6.1 Wind-dump Load Mechanical and Electrical Model

Synchronous generator: (salient pole)

$$\tilde{\omega}_s = \frac{1}{J_s}(-D_s\omega_s - T_s), \quad \tilde{\psi}_f = \frac{1}{\dot{\tau}_{do}}(-\psi_f + L_{md}i_{sd}) + e_{fd} \tag{A.1}$$

where $T_s = -\frac{L_{md}}{L_f}\psi_f i_{sq} - (\dot{L}_d - L_q)i_{sq}i_{sd}$

$$\begin{bmatrix} r_a & -\omega_s\dot{L}_d & 1 & 0 \\ \omega_s L_q & r_a & 0 & 1 \\ r_1 & -\omega_s L_1 & -1 & 0 \\ \omega_s L_1 & r_1 & 0 & -1 \end{bmatrix}\begin{bmatrix} i_{sd} \\ i_{sq} \\ V_{sq} \\ V_{sq} \end{bmatrix} + \begin{bmatrix} 0 & 0 \\ 0 & 0 \\ 1 & 0 \\ 0 & 1 \end{bmatrix}\begin{bmatrix} V_{dq} \\ V_{bd} \end{bmatrix} = \begin{bmatrix} \omega_s \frac{L_{md}}{L_f}\psi_f \\ 0 \\ 0 \\ 0 \end{bmatrix} \tag{A.2}$$

Drive train model

$$\begin{aligned} \tilde{\theta}_e &= \omega_{aref}(\omega_t - \omega_a) \\ \tilde{\omega}_t &= \frac{1}{J_t}\left(\frac{1}{2}C_p\rho A_r\frac{V_w^3}{\omega_t} - C_e\theta_e - (D_t + \omega_{aref}D_e)\omega_t + \omega_{aref}D_e\omega_a\right) \\ \tilde{\omega}_a &= \frac{1}{J_a}\left(C_e\theta_e + \omega_{aref}D_e\omega_t - (D_a + \omega_{aref}D_e)\omega_a - T_a\right) \end{aligned} \tag{A.3}$$

Induction generator: (cylindrical with short circuited rotor winding)

$$\tilde{\psi}_{rq} = \frac{1}{\dot{\tau}_o}(-\psi_{rq} + L_m i_{aq}) + \omega_{base}(\omega_s - \omega_a)\psi_{rd}$$
$$\tilde{\psi}_{rd} = \frac{1}{\dot{\tau}_o}(-\psi_{rd} + L_m i_{ad}) - \omega_{base}(\omega_s - \omega_a)\psi_{rq} \quad (A.4)$$

$$\begin{bmatrix} r_s & -\omega_s \dot{L}_s & 1 & 0 \\ \omega_s \dot{L}_s & r_s & 0 & 1 \\ r_2 & -\omega_s L_2 & (\omega_s^2 C_a L_2 - 1) & \omega_s r_2 C_a \\ \omega_s L_2 & r_2 & -\omega_s r_2 C_a & (\omega_s^2 C_a L_2 - 1) \end{bmatrix} \begin{bmatrix} i_{aq} \\ i_{ad} \\ V_{aq} \\ V_{aq} \end{bmatrix}$$
$$+ \begin{bmatrix} 0 & 0 \\ 0 & 0 \\ 1 & 0 \\ 0 & 1 \end{bmatrix} \begin{bmatrix} V_{bq} \\ V_{bd} \end{bmatrix} = \begin{bmatrix} \omega_s \frac{L_m}{L_r} \psi_{rd} \\ -\omega_s \frac{L_m}{L_r} \psi_{rq} \\ 0 \\ 0 \end{bmatrix} \quad (A.5)$$

Current balance from for electrical model

$$i_{sq} + i_{iq} - i_{lq} - i_{duq} = 0$$
$$i_{sd} + i_{id} - i_{ld} - i_{dud} = 0 \quad (A.6)$$

Where

$i_{iq} = i_{aq} + \omega_s C_a V_{ad}$, $i_{id} = i_{ad} - \omega_s C_a V_{aq}$,

$i_{duq} = V_{bq} / r_{dump}$, $i_{dud} = V_{bd} / r_{dump}$

$$i_{lq} = \frac{r_3}{r_3^2 + x_3^2} V_{bq} + \frac{x_3}{r_3^2 + x_3^2} V_{bd},$$

$$i_{ld} = -\frac{x_3}{r_3^2 + x_3^2} V_{bq} + \frac{r_3}{r_3^2 + x_3^2} V_{bd}$$

And

i_{iq}, i_{id}, i_{duq}, i_{dud} : current components of the load and dump load

V_{sq}, V_{sd}, V_{aq}, V_{ad} : stator terminal voltage components of SG and IG

e_{fd}, ψ_f : field voltage and field flux linkage of SG

ω_s : bus frequency (or angular speed of SG)

L_q, L_d : q-axis and d-axis inductance of SG

L_{md}, L'_d : d-axis field mutual and transient inductance of SG

L_f, L_m : field inductance and mutual inductance of SG

T_s, T_a : air gap torque of SG and IG

τ'_{do}, τ'_o : transient open circuit time constant of SG

i_{aq}, i_{ad} : stator phase current components of IG

ω_a, ω_t : rotational speed of IG and wind turbine

ψ_{rq}, ψ_{rd} : rotor flux linkage components of SG

C_a, r_{dump} : capacitor bank and dump load resistance

J_s, D_s : inertia and frictional damping of SG

r_s, r_a, L'_s, L_r : stator and rotor resistance and inductance of SG

r_1, r_2, L_1, L_2 : resistance and reactance between SG and bus and IG and bus

i_{sq}, i_{sd}, i_{iq}, i_{id} : current component of SG and IG into the bus.

6.2 Sliding Mode Controller

Equation (12) can be represented as

$$\dot{\breve{x}}_1(t) = \breve{A}_{11}\breve{x}_1(t) + \breve{A}_{12}\breve{x}_2(t)$$
$$\dot{\breve{x}}_2(t) = \breve{A}_{21}\breve{x}_1(t) + \breve{A}_{22}\breve{x}_2(t) + \breve{B}_2 u(t) \quad (B.1)$$

Where $\breve{x}_1 \in \Re^{(p+n-m)}$, $\breve{x}_2 \in \Re^m$, and $\breve{B}_2 \in \Re^{m \times m}$. The symmetric-positive definite matrix Q is

$$Q = \begin{bmatrix} Q_{11} & Q_{12} \\ Q^T{}_{12} & Q_{22} \end{bmatrix} \quad (B.2)$$

Where $Q \in \Re^{(p+n)\times(p+n)}$

(B.1) and (B.2) are substituted into (13), and the quadratic performance index is rewritten into the standard quadratic from such as

$$J = \frac{1}{2}\int_0^\infty \left(\hat{x}_1(t)^T \hat{Q}\hat{x}_1(t) + v(t)^T Q_{22} v(t)\right)dt \quad \text{(B.3)}$$

Where $\hat{Q}=Q_{11}-Q_{12}Q_{22}^{-1}Q_{21}$ and $v(t)=\hat{x}_2(t)+Q_{22}^{-1}Q_{21}\hat{x}_1(t)$.

Then, eliminating the $\hat{x}_2(t)$ contribution using $v(t)$ in (B.3), the modified state space model of (B.1) becomes

$$\dot{\tilde{x}}_1(t) = \hat{A}\hat{x}_1(t) + \breve{A}_{12}v(t) \quad \text{(B.4)}$$

Where $\hat{A} = \breve{A}_{11} - \breve{A}_{12}Q_{22}^{-1}Q_{21}$.

The problem thus becomes minimizing (B.3), subject to the system (B.4). A unique positive definite solution K is guaranteed by the algebraic Riccati equation [17] as

$$K\hat{A} + \hat{A}^T K - K\breve{A}_{12}Q_{22}^{-1}\breve{A}_{12}^T K + \hat{Q} = 0 \quad \text{(B.5)}$$

The simplest hyperplane system matrix S for the sliding mode controller is defined as

$$S = [S_1 \quad S_2] = [M \quad I_m] \quad \text{(B.6)}$$

Where $M = Q_{22}^{-1}\left(\breve{A}_{12}^T K + Q_{21}\right) \in \Re^{m\times(p+n-m)}$, $S_1 \in \Re^{m\times(p+n-m)}$, $S_2 \in \Re^{m\times m}$, and I_m is the identity matrix.

Once the hyperplane system matrix S is obtained in (B.6), a linear change of coordinate [15] is applied for presenting the control system as

$$\hat{G}\cdots\begin{bmatrix} I_{(p+n-m)} & 0 \\ S_1 & S_2 \end{bmatrix} \quad \text{(B.7)}$$

Where $I_{(p+n-m)}$ is the identity matrix and (B.7) is nonsingular, since S_2 is nonsingular. Let

$$\begin{bmatrix} \hat{x}_1(t) \\ s(t) \end{bmatrix} \cdots \hat{G}\begin{bmatrix} \hat{x}_1(t) \\ \hat{x}_2(t) \end{bmatrix} \quad \text{(B.8)}$$

Where $s(t)$ represents the switching function of the sliding mode controller and $s(t) = S_1\hat{x}_1(t) + S_2\hat{x}_2(t)$. The system (B.1) can be written with respect to these new coordinates as

$$\dot{\tilde{\hat{x}}}_1(t) = \overline{A}_{11}\hat{x}_1(t) + \breve{A}_{12}S_2^{-1}s(t) \quad \text{(B.9)}$$

$$\dot{\tilde{s}}(t) = S_2\overline{A}_{21}\hat{x}_1(t) + S_2\overline{A}_{22}S_2^{-1}s(t) + (S_2B_2)u(t) \quad \text{(B.10)}$$

Where $\overline{A} = \breve{A}_{11} - \breve{A}_{12}M$, $\overline{A}_{21} = M\overline{A}_{11} + \breve{A}_{21} - \breve{A}_{22}M$, and $\overline{A}_{22} = M\breve{A}_{12} + \breve{A}_{22}$.

The controllers are obtained from (B.10) as

$$(S_2B_2)u(t) = -S_2\overline{A}_{21}\hat{x}_1(t) - \left(S_2\overline{A}_{22}S_2^{-1} - \xi\right)s(t) \quad \text{(B.11)}$$

Where $\xi \in \Re^{m\times m}$ is any stable design matrix. Then, substituting $s(t)$ in (B.10) and the matrices $\overline{A}_{21}$ and $\overline{A}_{22}$, (B.11) can be rewritten for the proposed linear controller in (14) as

$$u(t) = -(S\breve{B})^{-1}(S\breve{A} - \xi S)\hat{x}(t) \quad \text{(B.12)}$$

Acknowledgment

The authors would like to gratefully acknowledge the financial support of KESRI (Korea Electrical Engineering & Science Research Institute) under project R-2007-1-015-02

References

[1] L. L. Feris, Wind Energy Conversion System, New Jersy: Prentice Hall, 1990.

[2] R. Hunter and G. Elliot, Wind-Diesel Systems, New York: Cambridge University, 1994.

[3] M. Sharaf and E. S. Abdin, " A digital simulation model for wind-diesel conversion scheme,"21th Southeastern Symposium on System Theory, 1989, pp. 160 - 66.

[4] K. Uhlen, B. A. Foss, and O. B. Gjosaeter, "Robust control and analysis of a wind-diesel hybrid power plant," IEEE Trans. on Energy Conversion, vol. 9, no.4, Dec. 1994, pp.701-708.

[5] R. B. Chedid, S. H. Karaki, and E. C. Chadi, "Adaptive fuzzy control for wind-diesel weak power systems," IEEE Trans. on Energy Conversion, vol. 15, no. 1, Mar. 2000, pp.71-78.

[6] G. S. Stavrakakis and G. N. Kariniotakis, "A general simulation algorithm for the accurate assessment of isolated diesel - ind turbines systems interaction: Part I: A general multigenerator power system model," IEEE Trans. on Energy Conversion, vol. 10, no.3, pp.577-583, Sept. 1995.

[7] G. S. Stavrakakis and G. N. Kariniotakis, "A general simulation algorithm for the accurate assessment of isolated diesel - ind turbines systems interaction: Part II: Implementation of the algorithm and case-studies with induction generators," IEEE Trans. on Energy Conversion, vol. 10, no.3, pp.584-590, Sept. 1995.

[8] T. S. Bhatti, A. A. F. Al-Ademi, and N. K. Bansal, " Dynamic and Control of isolated wind-diesel power system," International Journal of Energy Research, vol. 19, pp.729-740, 1995.

[9] J. Bowen, M. Cowie and N. Zakay, "The Performance of a remote wind-diesel power system," Renewable Energy of Elsevier Science Ltd., vol. 22, pp.429-445, 2001.

[10] G. Notton, C. Cristofari, P. Poggi, and M. Muselli, "Wind hybrid electrical supply system: behavior simulation and sizing optimization," Wind Energy, vol. 4, pp.43-59, 2001.

[11] S. C. Tripathy, M. Kalantar, and R. Balasubramanian, "Dynamics and stability of wind and diesel turbine generator with superconducting magnetic energy storage unit on an isolated power system," IEEE Trans. on Energy Conversion, vol. 6, no.4, pp.579-585, Dec. 1991.

[12] S. Borowy and Z. M. Salameh, "Dynamic response of a stand-alone wind energy conversion system with battery energy storage to a wind gust,"IEEE Trans. on Energy Conversion, vol. 12, no.1, pp.73-78, Mar. 1997.

[13] S. K. Aditya and D. Das, "Application of battery energy storage system to load frequency control of an isolated power system," International Journal of Energy Research, vol. 23, pp.247-258, 1999.

[14] P. Kunder, Power System Stability and Control, New York: McGraw-Hill, 1994.

[15] V. I. Utkin, J. Guldner, and J. Shi, "Sliding Modes in Electromechanical Systems, Philadelphia: Taylor and Francis, 1999.

[16] K. Tanaka and H. O. Wang, "Fuzzy Control Systems Design and Analysis, New York: John Wiley & Sons, 2001.

[17] K. Ogata, Modern Control Engineering, Upper Saddle River: Prentice-Hall, 1997.

[18] S. K. Bag, S. K. Spurgeon, and C. Edwards, "Output feedback sliding mode design for linear uncertain systems," Proceeding of IEE, Part D 144, pp. 209-216, 1997.

[19] G. Gu, "Stability conditions of multivariable uncertain systems via output feedback control," IEEE Trans. on Automatic Control 35, pp. 925-927, 1990.

[20] B. S. Heck, S. V. Yallapragada, and M. K. H. Fan, "Numerical methods to design the reaching phase of output feedback variable structure control," Automatica 31, pp.275-279, 1995.

[21] P. C. Krause, O. Wasynczuk, and S. D. Sudhoff, Analysis of Electrical Machinery, New York: McGraw-Hill, 1986.

[22] International Electrotechical Commision, Publication 34-10, Rotating electrical machines, Part 10: Conventions for description of synchronous machines, Geneve, 1975.

[23] Garduno-Ramirez R. and K. Y. Lee, "Power plant coordinated-control with wide-range control-loop interaction compensation" Proc. the 15th IFAC World Congress, (CD) paper #2407, 6 pages, Barcelona, Spain, July 21-26, 2002.

Biography

Won-Pyo Hong

Won-Pyo Hong received his B.S degree in Electrical Engineering from Sungsil University, Seoul, Korea, in 1978, his M.Sc. and Ph.D. degree in Electrical Engineering from Seoul National University, Seoul, Korea, in 1980 and 1989 respectively. From 1980 to 1993 he was employed as senior researcher number at the Power System Lab. of Kepri (Korea Electric Power Research Institute) in the Korea Electrical Power Company. From 1993, he is now a professor of the Department of Building Services Engineering at the Hanbat National University. His research activities are in the areas of the building and industrial application of field-bus, energy management, building automation and control, intelligent networked control, and control and planning of distributed energy resource.

Hee-Sang Ko

Hee-Sang Ko (St.M'8) received his B.S. degree in Electrical Engineering from Cheju National University, Korea, in 1996, and his M.S. degree in Electrical Engineering from the Pennsylvania State University in 2000. He has been working toward a Ph.D. in Electrical and Computer Engineering at the University of British Columbia since 2001. His research interests include power quality analysis of alternative energy systems and the estimation of power system data.